3rd EUropean Conference for Aero-Space Sciences, July 6-9th, 2009, Versailles – Paris, France

Wall Pressure and Thrust of a Dual Bell Nozzle in a Cold Gas Facility

P. Reijasse, D. Coponet, J.-M. Luyssen
ONERA, 92190, Meudon, France

V. Bar, S. Palerm, J. Oswald, F. Amouroux
CNES, 91023, Evry, France

J.-C. Robinet, P. Kuszla
ENSAM, 75000, Paris, France

Abstract

A dual bell nozzle has been tested in the ONERA-R2Ch wind tunnel within the CNES PERSEUS program. The wall pressure distributions and the thrust for the two flow regimes have been characterized in the nozzle pressure ratio (NPR) range from 51 up to 597. A hysteresis on the transition NPR between the two flow regimes has been observed according to the evolution of NPR. The duration for the switch between the two flow regimes is less than 10ms. The hysteresis of about 20% on the NPR is also directly applied to the thrust. The total thrust of the dual bell nozzle becomes higher than the base nozzle thrust for *NPR*>1500. The hysteresis phenomenon has been modeled with the use of supersonic separation criteria and by making the assumption that incipient separation occurs immediately after the transition for increasing NPRs, while effective separation is forming just before the transition for decreasing NPRs.

Notations

A_S	exit section
F	thrust
$\overline{F}$	normalized thrust by the thrust at the throat
J	junction
L	nozzle length
M	Mach number
NPR	Nozzle Pressure Ratio (=pt/pa)
p	pressure
R	radius

subscripts

1	base nozzle
2	nozzle extension
a	ambient
DB	dual bell
crit	critical (for NPR)
dec	decreasing (for NPR)
id	ideal (for a nozzle)
inc	increasing (for NPR)
int	intrinsic (for thrust)
t	total (for total pressure)
th	throat
tr	transition

Introduction

Within the PERSEUS program [1] driven by CNES, it is studied the possibility to equip a nanosatellite launcher with a dual bell nozzle. In order to better understand the aerodynamics of this nozzle concept a cold gas experimental study has been undertaken [2, 3]. The design method of the dual bell contour is presented. The wall pressure measurements and the thrust measurements are discussed. First RANS computations have been realized.

The dual bell nozzle is an auto-adaptive concept, first proposed in 1949 [4], relying on the altitude compensation. This concept uses a two section nozzle (Fig. 1). The first part of the divergent is the reference nozzle or the base nozzle. The second part is the nozzle extension. At the junction between the two sections there exists a discontinuity of wall slope –or wall inflection-.
In a dual bell nozzle there exists two flow regimes according to the nozzle pressure ratio (*NPR*) relatively to a critical value $NPR_{crit.}$ The nozzle pressure ratio is expressed as the ratio of the chamber pressure –or total pressure- over the ambient external pressure, $NPR = p_t / p_a$. As the chamber pressure of the engine is generally constant the NPR is continuously increasing during the ascent of the rocket.
The first flow regime (Fig. 2a) occurs for $NPR < NPR_{crit}$ at the lowest altitudes. Only the base nozzle is choked; the base nozzle is running in a full flow regime and the nozzle jet (Σ_j) separates at the junction J between the two sections. A typical wall pressure distribution corresponding to the first flow regime is given Fig. 3a. The pressure curve is characterized first by a decreasing due the expansion of the supersonic flow along the wall then by a rapid pressure rise induced by the shock to adapt the ambient pressure which is greater than the jet static pressure p_1 at the junction. The second part of the nozzle is fully separated and external air engulfs into the separation zone at a nearby ambient pressure value p_a.

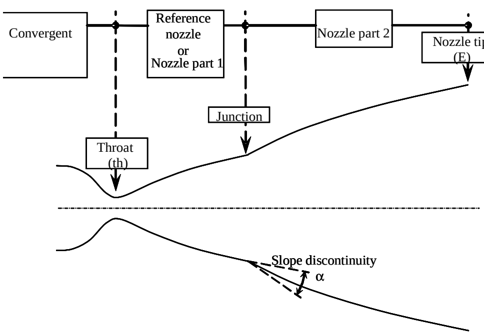

Fig. 1 – Nomenclature of a dual bell nozzle

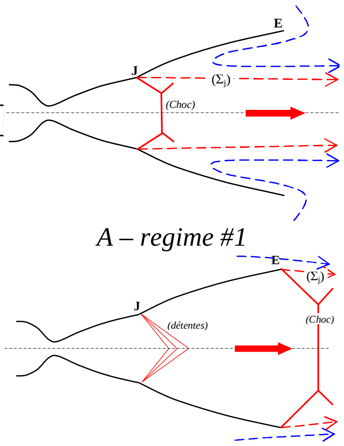

A – regime #1

B – regime #2

Fig. 2 – Schematic sketches of the two flow regimes

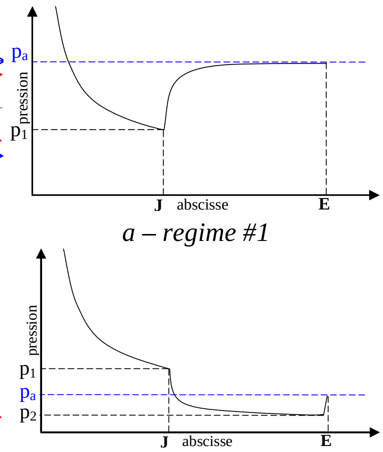

a – regime #1

b – regime #2

Fig. 3 – Typical wall pressure profiles of the two flow regimes

The second flow regime (Fig. 2b) occurs for $NPR > NPR_{crit.}$. The propulsive jet, after expanding at the junction, reattaches to the wall of the nozzle extension. Immediately after the transition the jet is overexpanded and separates at the nozzle lip E. The shock intensity issuing from the nozzle lip is equal to p_a / p_2 , where p_2 is the wall pressure of the nozzle extension in the attached boundary layer zone. As long as the pressure p_a will remain higher than the pressure p_2, the nozzle extension will be a source of drag. It is crucial to know at which NPR the whole dual bell nozzle will produce its maximum thrust.

Rapid bibliographical survey

The dual bell nozzle concept has gained renewed interest at the end of 1990's and early 2000's as a possibility to equip the engine of future space transport launch vehicles. In 2003 the Kakuda Space Centre of the Japanese agency JAXA considered this nozzle concept has prospects of being used for high-performance engines of reusable space vehicles [5]. The dual bell concept was under investigation in 2002 as a potential upgrade path for current launch vehicles by Boeing Rocketdyne [6]; the area ratios of the presented dual bell divergent were $\Sigma_1 \approx 25$ and $\Sigma_{DB} \approx 150$ and the lengths were respectively $L_1/R_{th} \approx 6$ and $L_{DB}/R_{th} \approx 16.6$. In 2002 European industry and the agency CNES have also envisaged the dual bell concept as a good candidate for improving the nozzle performances of the Vulcain rocket engine family [7]; this possibility was the conclusion of specific research efforts conducted in the frame of the joint cooperation FSCD program between Germany (ASTRIUM, DLR), Sweden (VOLVO Aero, SNSB, FOI) and France (CNES, SNECMA, ONERA) with the active contribution of ESTEC.
Different design aspects for the wall inflection and nozzle extension have been discussed in analytical and experimental German studies [8, 9, and 10] with special regard to the dependence of transition behavior from sea level to altitude operation on the type of nozzle extension. Several conclusions were derived from these studies. Two different types of nozzle extensions, the constant pressure extension and the overturned extension, might offer more rapid flow transition [8]. The losses caused by wall inflection have the same order of magnitude as the divergence loss of the reference bell nozzle. The application of commonly used separation criteria derived from conventional nozzles, gives reasonable results when applied to dual-bell nozzles [8]. The time needed for

the transition and the side loads induced by the transition have also been examined [9]. Typical timescales needed for the transition were less than 10ms for the constant pressure and for the overturned pressure contours. For both types of nozzle extensions, a strong hysteresis has been observed around the transition nozzle pressure ratio (NPR_{tr}) with a higher value for the start up. This hysteresis effect is found to be an obstacle for a potential pulsation between the two dual bell flow regimes [9]. The effect of the nozzle extension length onto the NPR transition and the transition time has been studied [10]. The appellation of the “sneak” transition –the phenomenon preceding the actual transition- has been given in [10] but this phenomenon was previoulsly characterized in [10] by the way of experiments and in [19] numerically.
The dual-bell transition has been numerically examined by several teams [11, 12 and 13] in order to re-build or to investigate the time needed for this transient phenomenon. The Baldwin-Lomax turbulent model has been employed in time-accurate computations for this dual bell transition problem [11]. The predicted transition duration agrees reasonably well with the experiments but the transition starts for a minimum pressure ratio of 10% higher than the experimental one. This discrepancy was attributed to compressibility effect not taken into account in the turbulent model [11]. A numerical study in 2005 [12] found that the deflection angle at the wall inflection should be larger than the angle determined by a Prandtl-Meyer expansion. Also this Japanese study has found that the time to accomplish the separation point transition from the wall inflection to the nozzle extension is less than 10ms when applied to the booster engine of H-2A launch vehicle. Another Japanese study [13] has experimentally investigated the flow transition by testing 9 dual-bell nozzles in a cold gas facility. “Instantaneous” movement of the separation point was found to occur during transition for dual bell nozzles with positive wall pressure gradient extension or with constant wall pressure gradient extension.

Design method of a dual bell nozzle contour

Pressure parameters of the dual bell nozzle

The apparition of the flow regimes will be determined by the values of the two jet pressure values p_1 and p_2 at the tip of the base nozzle –or at the junction- and at the tip the nozzle extension, respectively. Wall pressures p_1 and p_2 have been determined by F. Amouroux of CNES [14] in order to optimize the payload capability of the PERSEUS nanolauncher. It results from this optimization study the following values $p_1/p_t = 0.01252$ and $p_2/p_t = 0.00124$.

Base nozzle

The base nozzle profile is determined by using the inverse method of characteristics if one knows the boundary conditions at the inlet (transonic domain) and on the centerline [2].
The first step is to fix a curvature radius for the throat geometry then to calculate with a Euler code the transonic flow in this region (Fig. 4). A second step is to fix the boundary conditions for the next computation by the method of characteristics. These boundary conditions are the extraction of a starting characteristic line from the supersonic domain formerly computed and the building of pressure law on the centerline. The pressure law starts at the end of the transonic domain (point 00 on Fig. 5) and ends at the point which starts the constant Mach number zone. The third step is to calculate the characteristic mesh point by point and to extract the fluid perfect streamline issuing from a series of points P_i respecting the throat mass flow rate. The last step is the Euler computation of the whole ideal nozzle; the Euler computation can be compared with the method of characteristics (Fig. 6).

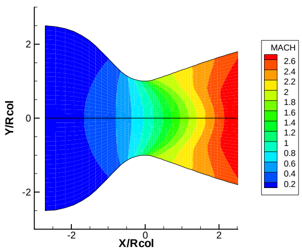

Fig. 4 – Transonic flow computed by an Euler code

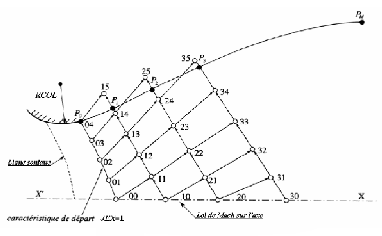
Fig. 5 – The inverse method of characteristics for the base nozzle contour

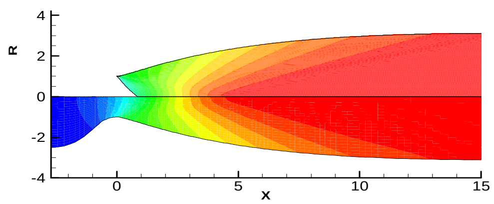

Fig. 6 – Mach number contour plot of the base nozzle; method of characteristics (top) and Euler (bottom)

The base nozzle is obtained by truncating the ideal nozzle at the wall abscissa where the pressure value p_1 is found. This corresponds to the Mach number M_1=3.53. The two parameters for studying the ideal nozzle are the exit Mach number M_{id} and the length of the ideal nozzle L_{id} issued from the length of the centerline pressure law. The range of Mach number M_{id} studied was from 3.6 to 3.9; the maximum value studied M_{id} =3.9 gives the best specific impulse. The Mach number M_{id} was limited to 3.9 because of the limitation of the exit radius. The ideal nozzle is truncated at L_1/R_{th}=8.833 (see Fig. 7). Table 1 summarizes the base nozzle characteristics.

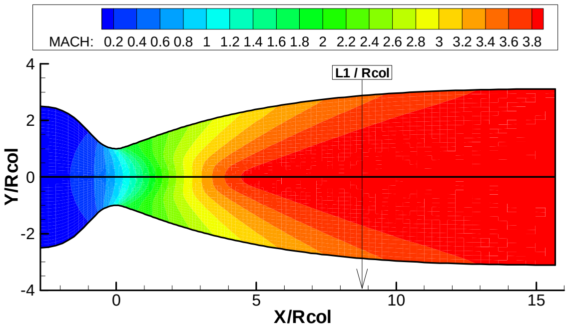

Fig. 7 - Base nozzle obtained by truncation of the ideal nozzle at L_1/R_{th}=8.833

		Ideal nozzle	Base nozzle
Isentropic pressure ratio at the exit	p1/pi		0,01252
Exit Mach number		3,9	3,533
Normalized specific impulse	Isp_1/Isp_throat	1,294	1,282
Nozzle length	$L_1/Rcol$	15,582	8,833
Exit radius	Y1/Rcol	3,106	2,879

Table 1 – Summarized characteristics of the base nozzle

Nozzle extension

The nozzle extension contour is defined to give a constant wall pressure p_2. For an inviscid fluid assumption this contour is coincident with an isobaric fluid-perfect streamline of pressure p_2. This streamline is obtained with the use of the direct method of characteristics by applying a centered expansion of intensity p_2/p_1 at the junction (Fig. 8). The computed iso-Mach number contour map is given Fig. 9.

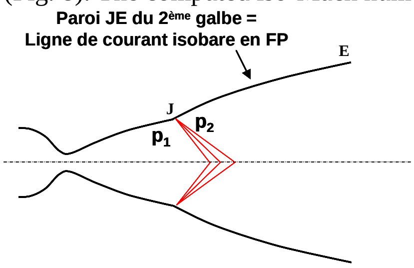

Fig. 8 – Centered expansion at junction J

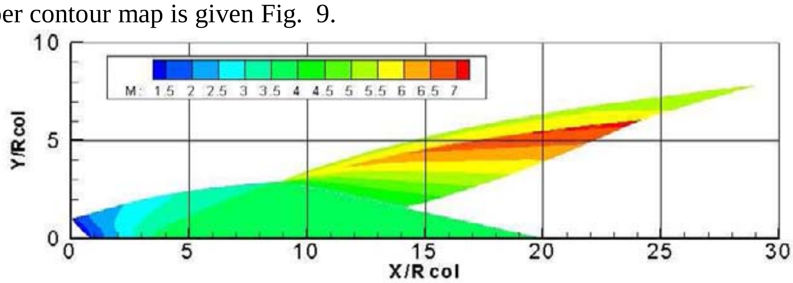

Fig. 9 – Supersonic Mach number contour plot of the dual bell nozzle with the use of the method of characteristics

The criterion retained for the nozzle extension length L_2 is the length ratio of the nozzle extension over the base nozzle L_2/L_1 chosen at a value of 2. The nozzle extension length L_2 is thus equal to 17.67.

Experimental set-up

Tests have been realized in the blow-down wind tunnel ONERA-R2Ch of Meudon Center [3]. A photograph and a sketch of the experimental set-up are presented in Figs. 10 and 11. The nozzle model is fixed on a cylindrical tube which is an interface between the model and the balance. The tube consists in a chamber which is supplied with compressed air by the use of four feeding pipes. The feeding pipes are positioned perpendicularly to the thrust axis.

Fig. 10 – The dual bell nozzle model in the ONERA R2Ch test chamber

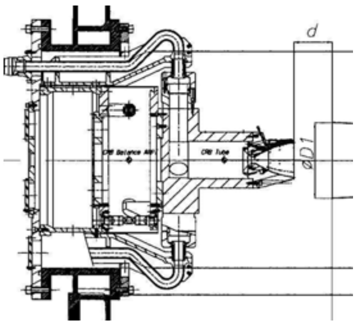

Fig. 11 – Sketch of the experimental set-up

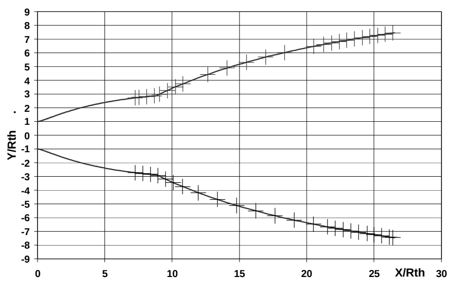

Fig. 12 – Internal dual bell contour and wall pressure tap positions (+)

Normalized by the throat radius, the convergent part of the nozzle model is 5.68*R_{th} long, and the dual bell diverging part is 26.51*R_{th} long. The exit diameter is 14.92*R_{th}. Forty-eight pressure taps are distributed onto two generating opposite lines (see Fig. 12).

The efforts and moments have been measured with a 6-component wall balance containing three axial dynamometers and three transverse dynamometers.

Test results

NPR stabilization

The objective of this test campaign is to characterize the wall pressure distributions and the axial thrust of the dual bell nozzle model according to varying NPR in steady regime. The total pressure of the nozzle jet is constant and fixed to $p_t \approx 52x10^5$Pa.

The variation of NPR is obtained by the variation of the ambient pressure p_a in the test chamber. Three combined ways were used to induce the variation of pa. The first one is to change the geometry of the supersonic ejector (diameter, cone angle, distance from the nozzle exit), the second one is to manage an entering mass flow rate into the test chamber through an opening controlled by a valve, and the last one is to vary the initial pressure value in the test chamber.

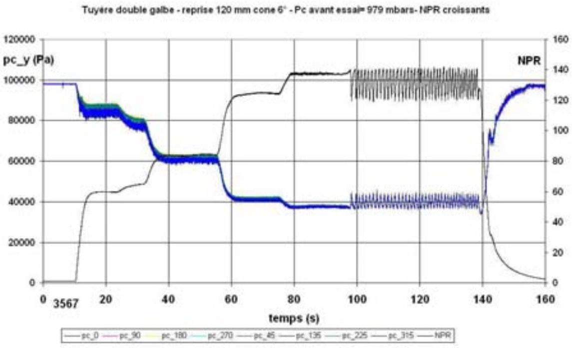

Fig. 13 – Ambient pressure and NPR evolutions versus time (test with increasing NPR)

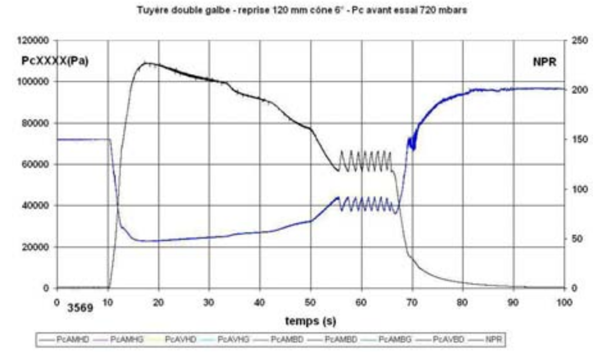

Fig. 14 – Ambient pressure and NPR evolutions versus time (test with decreasing NPR)

With these methods it has been possible to stabilize the lowest values of NPRs in the range 50<NPR<130 (see for instance Fig. 13). For NPRs>130 it was not possible to perfectly stabilize them even with the smallest ejector diameter tested (See Fig. 13).

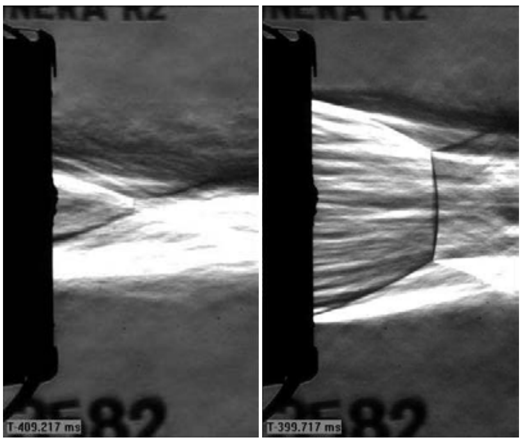

Regime#1 Regime#2

Fig. 15 - Switch regime#1 ➔ regime#2 at about NPR=130 (duration of switch less than 10ms)

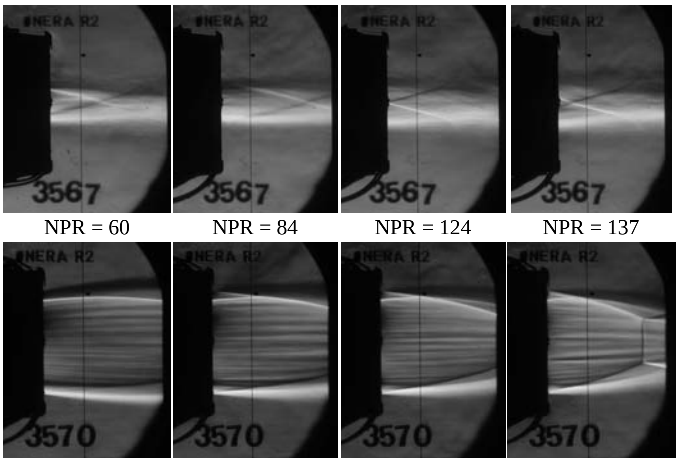

NPR = 60 NPR = 84 NPR = 124 NPR = 137

NPR = 577 NPR = 406 NPR = 317 NPR = 221

Fig. 16 – Series of schlieren photographs of the dual bell nozzle jet ; Regime#1 with NPR increasing (top) and regime#2 with NPR decreasing (bottom)

A series of schlieren photographs of the dual bell nozzle jet for the two flow regimes are shown Fig. 16.

When NPR increases and it approaches the value 140, a phenomenon inducing periodic oscillations of the ambient pressure appears (see Fig. 13). At first one can see weak oscillations at NPR=137 for t<95s. At this NPR wall pressure signals immediately after the junction were also characterized by strong amplitude oscillations. The first regime of oscillations can be attributed to the beginning of a sneak transition as mentioned in [10]. A second regime of oscillations, with a bigger amplitude between NPR=140 and NPR=120, is observed for t>100s; the apparent frequency is about 1Hz. This range of NPR oscillations corresponds to the switch domain range from regime#1 to regime#2. This oscillation frequency is apparent because it is given by steady pressure taps. In fact the switch phenomenon is much more rapid than 1Hz; it occurs in a duration time less than 10ms as it has been observed on schlieren photographs Fig. 15. One can also notice that the first oscillation begins at the highest value NPR=140 (see Fig. 13).

For NPR decreasing, the same type of oscillations occurs when NPR approaches the switch domain. The first oscillation begins at the lowest value, NPR=120 (see Fig. 14).

Vacuum pressure profiles

The dual bell contour has been determined by the use of an inviscid method. No boundary layer correction has been made for the wall. One can see, Fig. 20, the wall pressure distributions issued from the method of characteristics (*see blue line*) and computed by a RANS code *(see red line*); these computations can be compared with the experimental data for the highest NPR tested (*NPR*=435). Some discrepancies appear for the method of characteristics around the junction; this is due to the fact that the inviscid method uses a centered expansion at the junction while the real flow develops a boundary layer which smoothes the geometrical singularity. Another small difference appears for both computations as they cannot reproduce a slight augmentation of the measured wall pressure on the nozzle extension near the extremity. The measured pressure value is $\overline{p}_2$ =0.00164 instead of $\overline{p}_2$ =0.00124 predicted by the Euler method. This slight overpressure can be due to a beginning of air condensation knowing that the nozzle jet Mach number is M_2=5.34 and that the total temperature is about 330K.

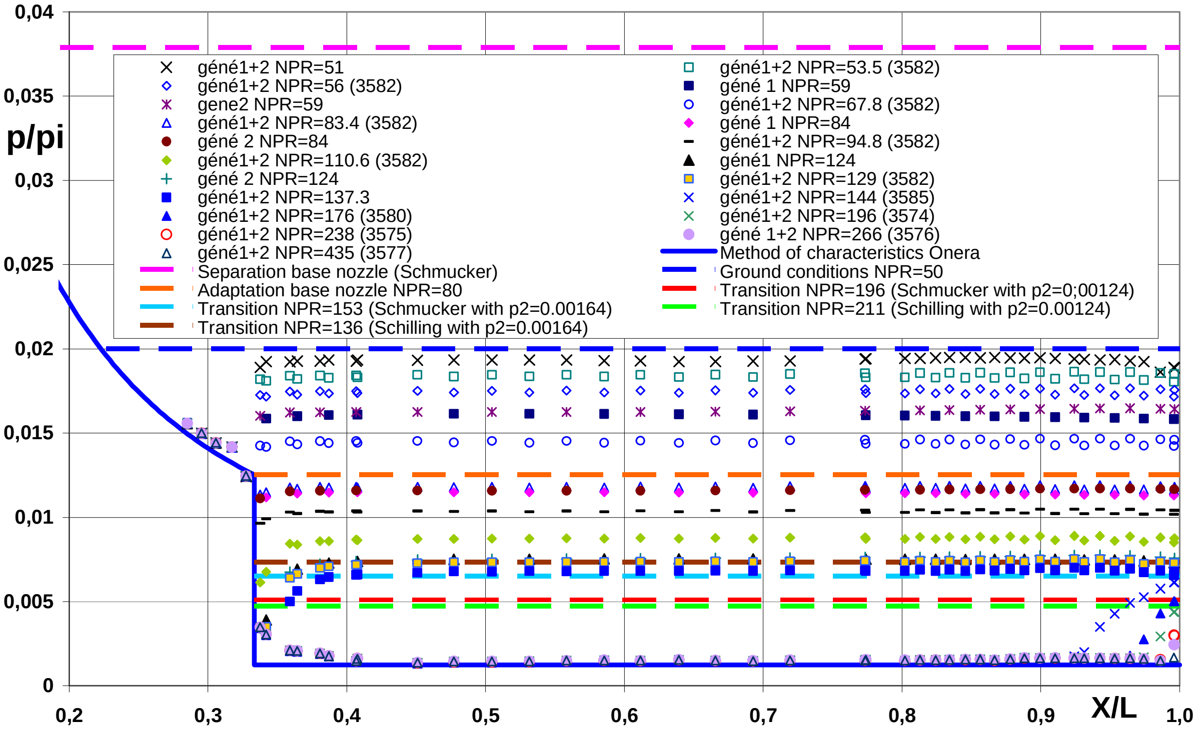

Wall pressure profiles around the transition regime#1 – regime#2

The adaptation of the base nozzle during regime#1 is obtained at *NPR*=80. For NPRs>80 one can see Fig. 17 that the flow expands at the junction just before crossing a separation shock. The rapid expansion is called in ref [10] the sneak transition.

For ground conditions, the atmospheric pressure being 1bar, the nozzle pressure ratio will be *NPR*=50 (*see dashed line in blue*, Fig. 17); the base nozzle will run in slight overexpanded flow regime. Nevertheless, this overexpansion regime will not induce an extended flow separation (i.e. with external recirculating air inside the base nozzle) because it might be an expansion ratio *NPR*=26 according to the Schmucker criterion [15] (*see dashed line in rose*, Fig. 17).

The transition regime#1 – regime#2 occurs in the NPR range from 138 up to 144 according to the experiments. A method to estimate the transition NPR while NPR is increasing ($NPR_{tr,inc}$) is to assume that, immediately after the transition, the nozzle extension flow is overexpanded with an incipient separation at the nozzle extremity. Let us consider two supersonic flow separation criteria:

- the Schmucker criterion, $\dfrac{p_a}{p_2} = (1{,}88\, M_2 - 1)^{0{,}64}$ where p_2 is the vacuum wall pressure on the nozzle extension ;
- the Schilling criterion [16], $\dfrac{p_2}{p_i} = 0{,}582\left(\dfrac{p_i}{p_k}\right)^{-1{,}195}$ where p_k is the pressure in the separated region, not too far from the external or ambient pressure.

With the pressure value predicted by the inviscid method p_2=0.00124, the Schmucker criterion and the Schilling criterion give the following NPR transition values, $NPR_{tr,inc}$=196 and $NPR_{tr,inc}$=211, respectively ; these NPR_{tr} values are higher the experimental ones. In other words the transition is predicted too late (*see dashed lines in orange and green*, Fig. 17). If one considers the measured value of the wall pressure p_2 (p_2=0,00164), one finds predicted transition NPR values closer to the experimental ones, $NPR_{tr,inc}$=153 and $NPR_{tr,inc}$=136, respectively (*see dashed lines in blue and brown*, Fig. 17).

Thrust and hysteresis

Regime#1

The intrinsic thrust $F_{\text{int},1}$ of regime#1 is computed by the use of an axisymmetric Euler code; the intrinsic thrust normalized by the thrust value at the throat F_{th} is equal to $\overline{F}_{\text{int},1} = F_{\text{int},1} / F_{th} = 1{,}282$. The thrust at the throat F_{th} is deduced from the isentropic relation with a Mach number equal to 1. The real thrust $F_{real,1}$ during regime#1 is obtained by the relation $F_{real,1} = F_{\text{int},1} - \dfrac{p_i}{NPR}.A_{S1}$, where A_{S1} is the exit section of the base nozzle. The thrust evolution of regime#1 is plotted Fig. 18a according to NPR.

Regime#2

The intrinsic thrust $F_{int,2}$ provided by the nozzle extension alone has been evaluated by the method of characteristics. We found $\overline{F}_{\text{int},2} = F_{\text{int},2} / F_{th} = 0.0242$. The total intrinsic thrust $\overline{F}_{\text{int},DB}$ normalized par F_{th} is thus equal to $\overline{F}_{\text{int},DB} = \overline{F}_{\text{int},1} + \overline{F}_{\text{int},2} = 1.3062$. So, the total real thrust of the dual bell nozzle according to the NPR is equal to $F_{real,DB} = F_{\text{int},DB} - \dfrac{p_i}{NPR}.A_{S2}$, where A_{S2} is the exit section of the base nozzle. The thrust evolution of regime#2 is plotted Fig. 18a according to NPR.

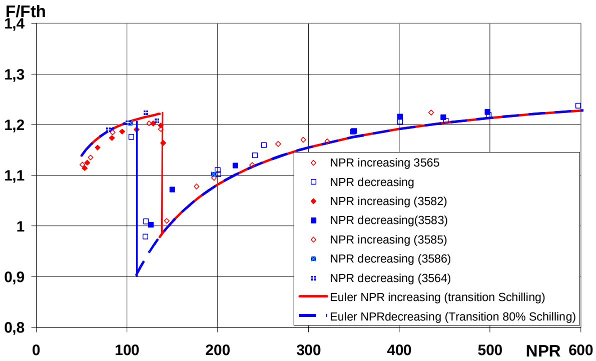

a – hysteresis modeling with the use of supersonic separation criteria

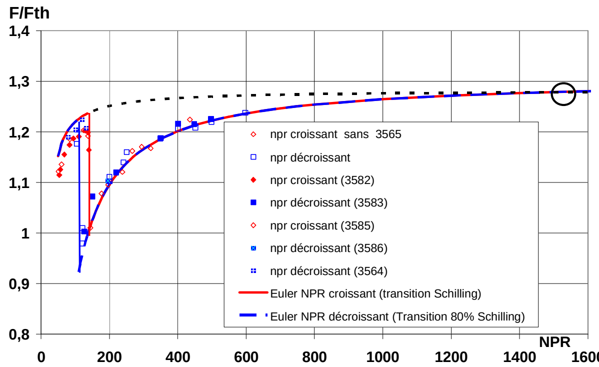

b – recovery of the base nozzle thrust at NPR=1500

Fig. 18 – Normalized thrust versus NPR. Increasing NPR in red, decreasing NPR in blue.

Transition

The transition from regime#1 to regime#2 while NPR is increasing, occurs at $NPR_{tr,inc}$=136 for the Schilling criterion and at $NPR_{tr,inc}$=153 for the Schmucker criterion. The transition given by the Schilling criterion is plotted in Fig. 18a (*red line*). For decreasing NPRs the measurements give a transition from regime#2 to regime#1 at a NPR value comprised between 120 and 104.

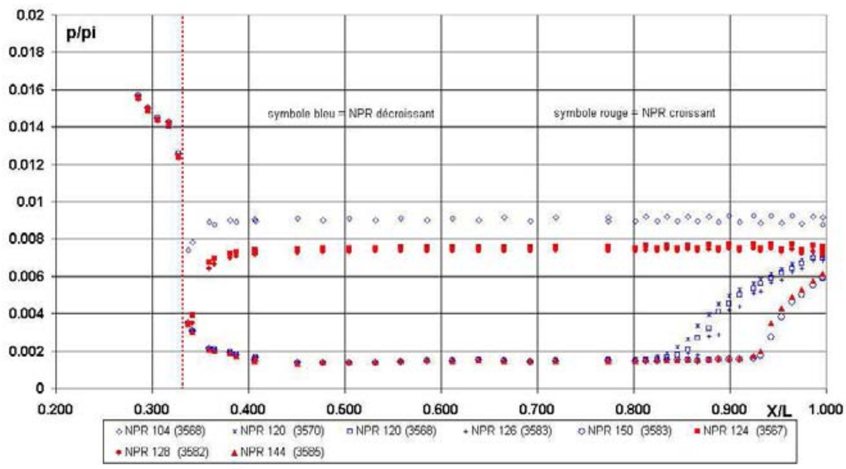

Fig. 19 – Hysteresis effect on the wall pressure at the extremity of the nozzle extension.
NPR increasing (red symbols) ; NPR decreasing (blue symbols)

This hysteresis is interpreted with the following assumption. Immediately after the transition while NPR is increasing, the flow at the extremity of the nozzle extension is in overexpansion regime with an incipient separation; the incipient separation is assumed to be predicted by the criteria mentioned above. Just before the transition while NPR is decreasing, the boundary layer resists to the adverse pressure gradient up to the creation of an effective separation with the onset of a plateau pressure. The shape differences of the wall pressure distributions for the two types of transition are well visible in Fig. 19; these shape differences consolidates the assumption of the two types of flow separation, before and after the transitions.
The pressure gradient difference between an incipient separation and an effective separation can be expressed with the use of separation criteria issued from a study performed by Zukoski [17] on the supersonic separation properties. For our study the pressure gradient is expressed by the ratio p_a / p_2 . The separation criteria are:

- Incipient separation criterion: $\frac{p_k}{p_2} = 1 + 0{,}73 \frac{M_2}{2}$
- Effective separation criterion: $\frac{p_a}{p_2} = 1 + \frac{M_2}{2}$

In our study the Mach number M_2 is equal to 5.34. This gives a 25% stronger intensity of the pressure gradient for the transition when NPR is decreasing. This corresponds to a transition value $NPR_{tr,dec}$ 20% less strong than the $NPR_{tr,inc}$. So the values of NPR transition while NPR is decreasing are: $NPR_{tr,dec}$=108 (Schilling) and $NPR_{tr,dec}$=122 (Schmucker). The NPR transition values deduced from the Schilling's criterion are plotted Fig. 18a.
Finally the transition regime induces a loss of thrust. The total thrust of the dual bell nozzle becomes higher than the base nozzle thrust for *NPR*>1500 as shown in Fig. 18b.

RANS computations

First steady Navier-Stokes axisymmetric computations have been done by ENSAM [18] with Fluent code at NPR=400. The turbulence model is the k-ω SST model. The size of the computational domain is 8*L_{DB} long and 4.5*L_{DB} high. Three grids were used (X1mesh: 120 000cells; X4 mesh: 500 000cells and X16 mesh: 2millions cells). The grid convergence has been obtained for X4 and X16 grids. The smallest values of Y^+ were 35 for X4 grid and 16 for X16 grid. The computed wall pressure profile is shown in Fig. 20. One can see a good re-building of the wall pressure. The Mach disk pattern has been obtained only for X4 mesh and for X16 mesh (see Fig. 21). One can notice that the Mach disk pattern was visualized at NPR=221 in Fig. 16. Further steady and unsteady computations are planned, in particular around the transition NPRs.

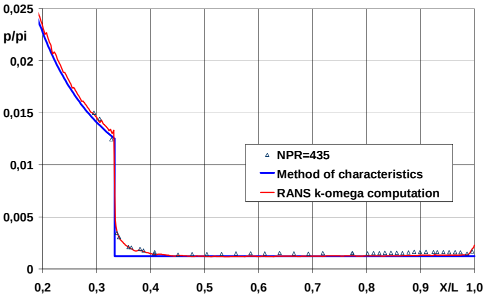

Fig. 20 – Wall pressure profile. NPR=400. Fluent code.

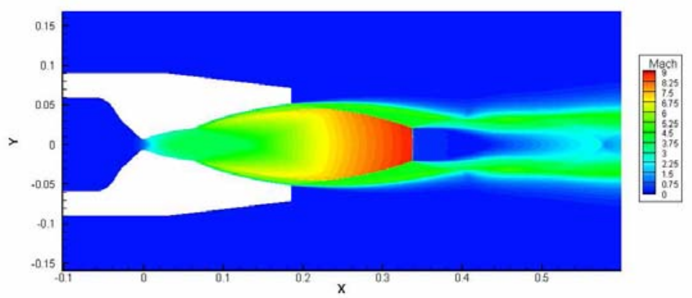

Fig. 21 – Iso Mach number contour plot. NPR=400. Fluent code

Conclusions

The test campaign realized in the ONERA-R2Ch wind tunnel has determined the aerodynamic behavior of a dual bell nozzle subscale model. The wall pressure distributions for the two flow regimes have been characterized in the nozzle pressure ratio (NPR) range from 51 upto 597. A hysteresis on the transition NPR between the two flow regimes has been observed according to the evolution of NPR.
The transition occurs at about NPR=140 while NPR is increasing and at about NPR=120 while NPR is decreasing. The duration for the switch between the two flow regimes is less than 10ms.
The wall pressure values predicted by the Euler method are in good agreement with the measured pressure data. Nevertheless small discrepancies appear at the junction because the modeling with the use of a centered Prandtl-Meyer expansion does not reproduce the viscous phenomena of the boundary layer which smoothes the geometrical singularity. Another small difference appears with the wall pressure level on the nozzle extension; the slight overestimation of the fluid perfect wall pressure in the final part of the nozzle can be due to a beginning of air liquefaction as the Mach number is 5.34 and the total temperature is about 330K.

An estimation of the nozzle thrust has been made with the Euler method. The thrust values are normalized by the thrust produced at the throat region. The hysteresis of about 20% on the NPR is also directly applied to the thrust. The total thrust of the dual bell nozzle becomes higher than the base nozzle thrust for *NPR*>1500.
The hysteresis phenomenon relies on the assumption that incipient separation occurs immediately after the transition for increasing NPRs, while effective separation is forming just before the transition for decreasing NPRs.

References

[1] R. Bec, C. Bernard-Lepine, K. de Groote and F. Amouroux, *PERSEUS. A Nanosatellite Launch System Project Focusing on Innovation and Education*, 2nd EUropean Conference for AeroSpace Sciences (EUCASS), Liège (BE), July 2007.

[2] P. Reijasse , *Conception d'un profil de tuyère double-galbe. Programme PERSEUS. (In English : Design of a dual bell nozzle contour. PERSEUS program)*, ONERA RT 1/14512 DAFE, February 2009.

[3] D. Coponet and P. Reijasse, *Projet PERSEUS. Etude expérimentale de la poussée d'une tuyère double galbe. Soufflerie R2Ch. (In English : PERSEUS project. Experimental study of the thrust of a dual bell nozzle)*, ONERA RT 2/14512 DAFE, June 2009.

[4] C. Foster and F. Cowles, *Experimental Study of Gas-Flow Separation in Overexpanded Exhaust Nozzles for Rocket Motors*, Jet propulsion Lab., Progress Rept. 4-103, California Inst. of Technology, Pasadena, CA, 1949.

[5] JAXA/Kakuda Space Center web site. « Combustor and Nozzle section », 2003.

[6] L. Haas, *Liquid Rocket Engine Nozzles*, Boeing/Rocketdyne P&P, Presentation to UCLA class, June 2002.

[7] B. Stephan, A. Beaurain, M. Pons, D. Preclick, A. I. Pettersson and M. Gruslin, *Technology Demonstrators for Vulcain 3 Engine*. 2002

[8] M. Frey and G. Hagemann, *Critical Assessment of Dual-Bell Nozzles*, Journal of Propulsion and Power, Vol. 15, No. 1, January-February 1999.

[9] G. Hagemann, M. Terhardt, D. Haeseler and M. Frey, *Experimental and Analytical Design Verification of the Dual-Bell Concept*, Journal of Propulsion and Power, Vol. 18, No. 1, January-February 2002.

[10] C. Nürnberger-Genin and R. Stark, *Flow Transition in Dual bell nozzles*, Shock Waves DOI 10.1007/s00193-008-0176-4, © Springer-Verlag 2008.

[11] H. Wong and R. Schwane, *Numerical Investigation of Transition in Flow Separation in a Dual-Bell Nozzle*, Proc. 4th European Symposium on Aerothermodyanmics for Space Applications, 15-18 Oct. 2001, Capua Italy, ESA SP-487, March 2002.

[12] H. Otsu, M. Miyazawa and Y. Nagata, *Design Criterion of the Dual-Bell Nozzle Contour*, IAC-05-C4.2.08

[13] T. Tomita, M. Takahashi, M. Sasaki and H. Tamura, *Investigation on Characteristics of Conventional-Nozzle-Based Altitude Compensating Nozzles by* Cold-Flow Tests, 42nd AIAA/ASME/SAE/ASEE Joint Propulsion Conference & Exhibit, 9-12 July 2006, Sacramento (CA), USA, 2006; AIAA 2006-4375.

[14] F. Amouroux, *Optimisation des rapports de section d'une tuyère à double galbe (In English: Optimization of the area ratios of a dual bell nozzle) (PERSEUS)*, CNES PER-NT Ed. 1 Rév. 1, 10/07/2008.

[15] R. Schmucker, *Status of flow separation prediction in liquid propellant rocket nozzle*, NASA TM X-64890, Nov. 1974.

[16] M. Schilling, *Flow separation in a rocket nozzle*, M.S. thesis, University of Buffalo, June 1962.

[17] E. Zukoski, *Turbulent boundary layer separation in front of a forward-facing step*, AIAA Journal, Vol.5, n°10, Jan. 1967.

[18] P. Kuszla, *Preliminary Dual bell nozzle RANS computations at NPR=400*, Perseus technical meeting presentation, june 2009.

[19] F. Nasuti and M. Onofri, *Flow analysis and methods of design for dual-bell nozzles*, AIAA 2001-3558